Supporting Information

Highly Tough Hydrogels with Body Temperature-Responsive Shape Memory Effect

Ruixue Liang[†], *Haojie Yu*[†,*], *Li Wang*[†,*], *Long Lin*[‡], *Nan Wang*[†], *Kaleem-ur-Rahman Naveed*[†]

[†]State Key Laboratory of Chemical Engineering, Institute of Polymer and Polymerization Engineering, College of Chemical and Biological Engineering, Zhejiang University, Hangzhou 310027, China

[‡]Department of Colour Science, University of Leeds, Woodhouse Lane, Leeds LS2 9JT,

Corresponding authors: Haojie Yu Email: hjyu@zju.edu.cn

Li Wang Email: opl_wl@dial.zju.edu.cn

Dynamic mechanical analysis (DMA)

Thermal-mechanical tests were performed on a Q800 dynamic mechanical analyzer (TA instrument, USA) under the tensile mode, fixed frequency of 1Hz, amplitude of 20 μm, heating rate of 2 ^{o}C/min and a temperature range of 10 to 60 ^{o}C. All the samples were cut into uniform rectangle-shaped specimens (30 mm×5 mm×1 mm) and coated with silicone grease.

Fourier-transform infrared spectroscopy (FTIR)

FTIR spectra were measured on a Nicolet 5700 spectrometer (ThermoNicolet Corporation, USA), samples were completely dried before test.

Thermogravimetric analysis (TGA)

TGA was performed on a Q500 thermo-analyzer instrument (TA, USA) from 50 to 800 ^{o}C at a linear heating rate of 10 ^{o}C/min under a nitrogen flow.

Wide-angle X-ray diffraction (WAXD)

WAXD measurements were performed on an X'pert powder diffractometer (PANalytical, Netherlands) with Cu-Kα radiation (λ = 0.15418 nm). Measurements were carried out in the 2θ range 5 to 80° using a step size and a step time of 0.026° and 27.54 s, respectively. Samples were completely dried before the tests.

Scanning electron microscopy (SEM)

The micro-structures of the hydrogels were determined by SEM (Zeiss, Utral 55). All the hydrogel samples were freeze-dried before the tests.

Quantitative evaluation of the shape memory performance

As shown in scheme S1 : (Step 1) A straight strip of hydrogel specimen was immersed in 37 ºC DI water for 10s and then was folded into a U-shape by applying external force at the soft state. (Step 2) The folded specimen was taken out of the 37 ºC DI water and immediately immersed in 10 ºC DI water for 10 s to fix the temporary shape. The recovery angle and the fixed temporary angle were defined as α and 180-α, respectively. (Step 3) The bended specimen was taken out from the cold water with a tweezers and then re-immersed in the 37 ºC DI water. (Step4) After re-immersing the specimen in 37 ºC water, the temporary shape was recovered gradually. The recovery time and the residual angel (β) were record. The shape fixity (R_f) and shape recovery (R_r) were quantitatively determined by following equations according to Bai *et al.* [1]

$$R_f = \frac{180-\alpha}{180} \times 100\%, \quad R_r = \frac{180-\alpha-\beta}{180-\alpha} \times 100\%$$

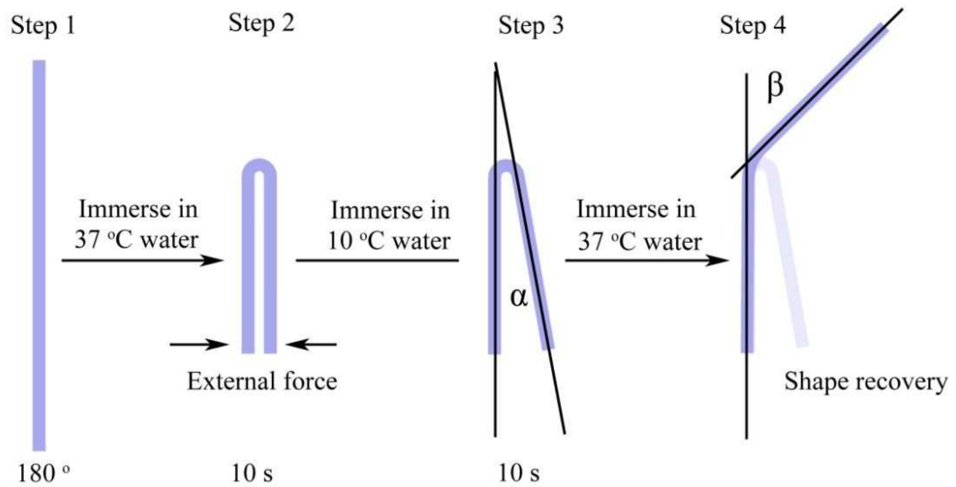

Scheme S1 Schematic illustration of the shape memory behavior test

Cell viability assay

The cytotoxicity of the hydrogel P60-A40 was assessed *in vitro* through a Cell Counting Kit-8 (CCK-8) assay on 4T1 breast cancer cells. 4T1 cells were seeded in 96-well plate at a density of 1.0×10^4 cells/well in 100 μl RPMI-1640 medium supplemented with 10% fetal bovine serum, 100U/ml penicillin, and 100 μg/ml streptomycin, and allowed to attach for 24h at 37 ^oC with 5% CO_2. The sterilized hydrogel sample was immersed in the culture medium at extraction ratios of 0, 5, 10, 15 and 20 mg/ml for 24 h at 37 ^oC to obtain the extracts. The culture medium in the wells was removed and replaced by the extracts. After incubation of the cells with the extracts at 37°C for 24h, CCK-8 (10 μl) was added to each well, and the cells were continuously incubated for another 1 h at 37 ^oC. Finally, the cell viability was determined by recording the absorbance at 450 nm using a microplate reader.

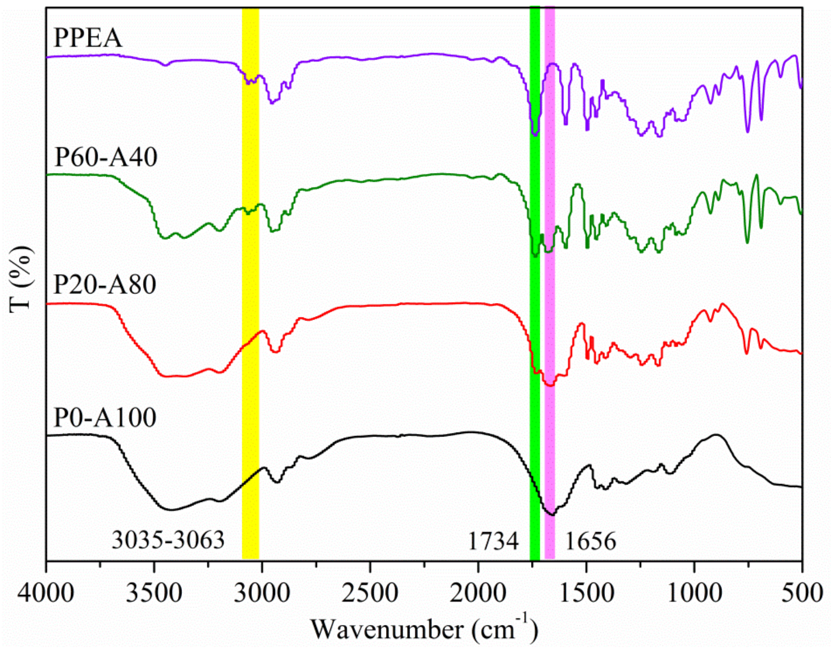

Figure S1 FTIR spectra of dried P0-A100, P20-A80, P60-A40 hydrogels and PPEA

Amide hydrogen bonds and hydrophobic interactions are dissociated in DMSO, thereby, the network of the organogel was connected only by the chemical crosslinks, PEGDA700. The photo demonstration in Figure S2 proves that no physical crosslinks formed without water treatment.

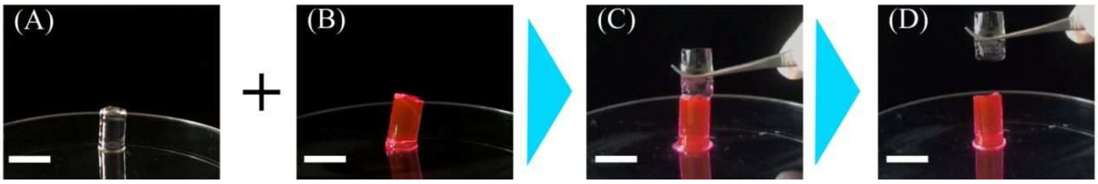

Figure S2 Images demonstrating two halves of P60-A40 organogel in (A) and (B), respectively, being brought into contact for a while at their fully DMSO swollen state, and no welding was observed. (C) Attachment of the two halves. (D) Lifting one half by a tweezers, and the two halves still remained in a separate state. The sample in (B) was dyed with rhodamine B for better observation, scale bar: 1cm.

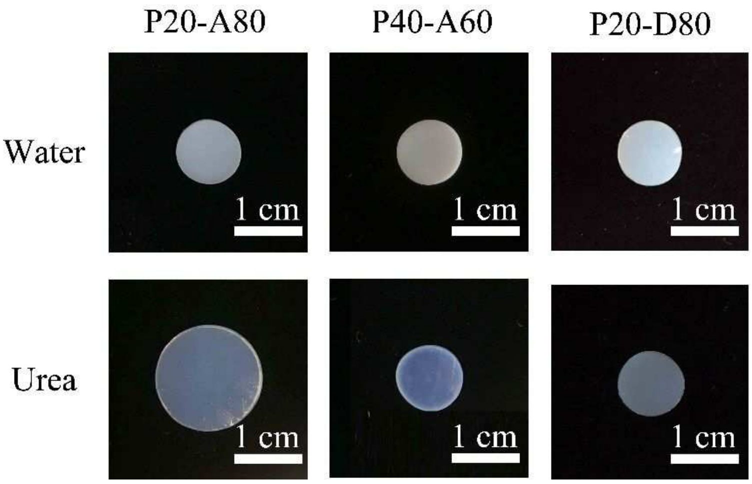

Figure S3 The swelling behavior of hydrogels P20-A80, P40-A60 and P20-D80 in water and 5M urea solution, respectively, at 25 ^{o}C.

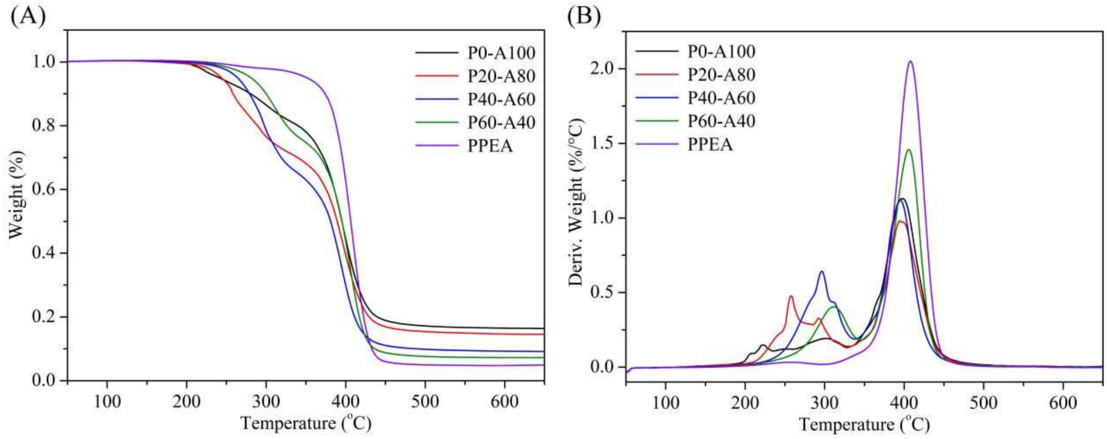

Figure S4 Thermogravimetric analysis of the dried hydrogels and PolyPEA. (A) The TG curves and (B) the corresponding DTG curves.

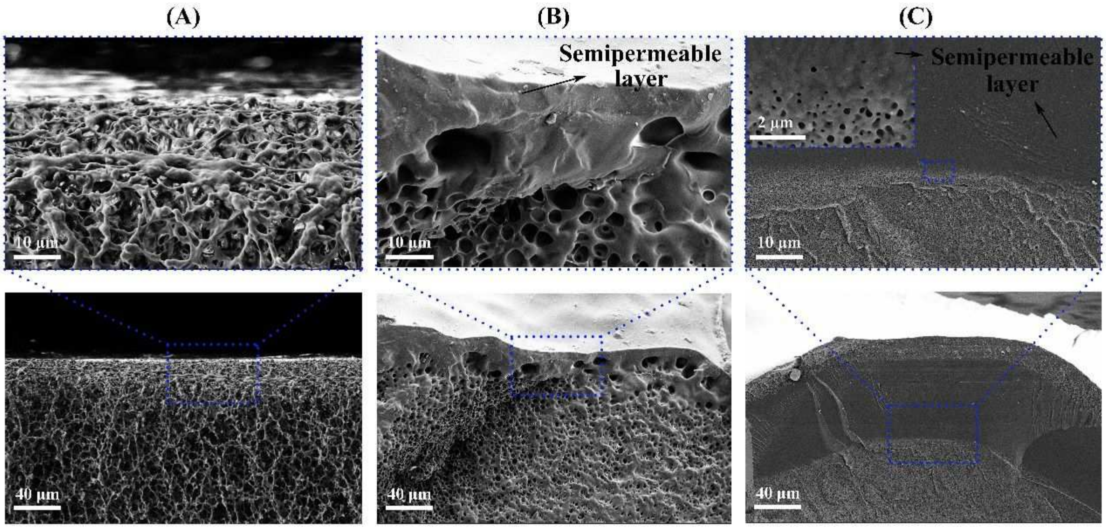

Figure S5 Microscopic structure of the cross-sections of the freeze-dried hydrogels at various magnifications. (A) P0-A100, (B) P20-A80, (C) P60-A40.

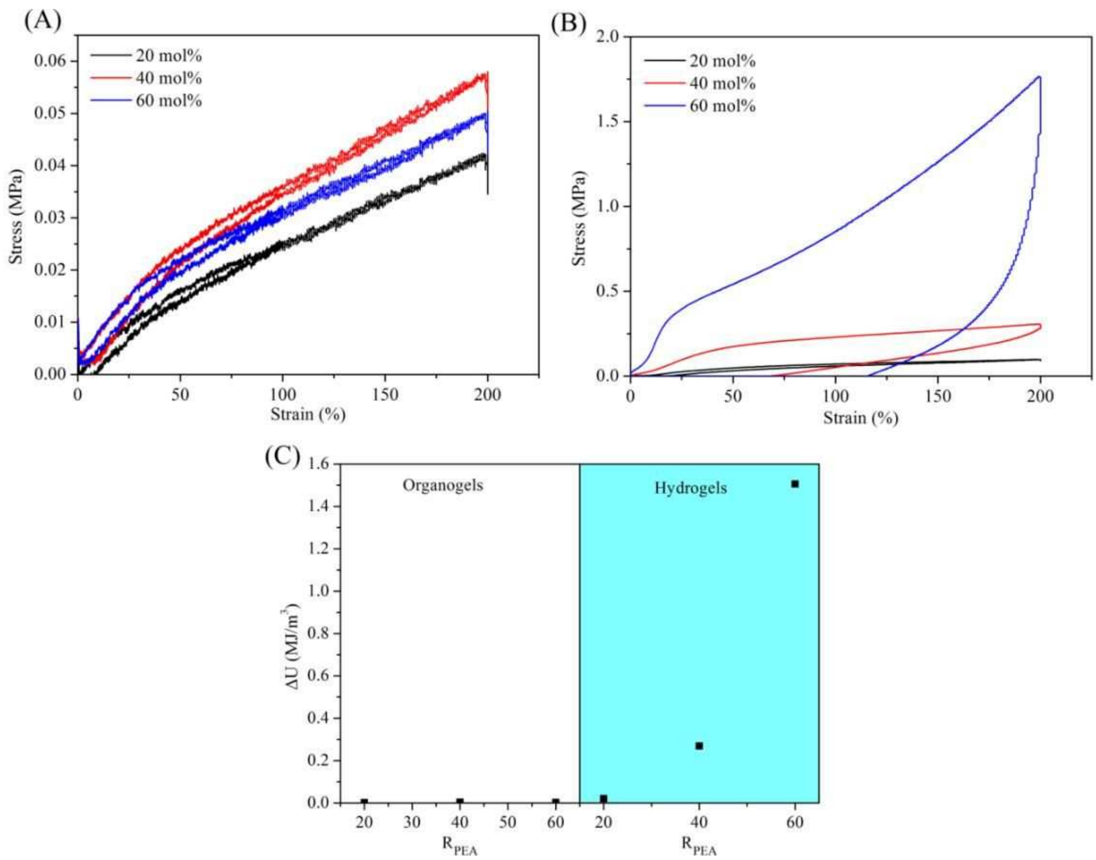

Figure S6 Samples of the (A) as-prepared organogels and (B) the corresponding hydrogels with different R_{PEA}=20, 40 and 60 were subjected to a cycle of loading and unloading to fixed strain. (C) The dissipated energy (ΔU) during the tensile loading-unloading tests of as-prepared organogels and hydrogels with strong dependence on $R_{PEA.}$

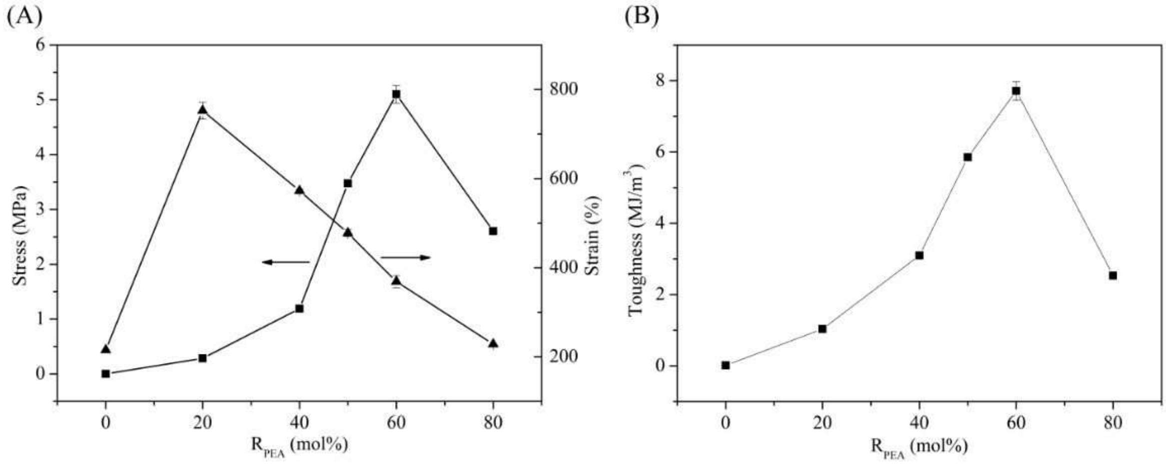

Figure S7 (A) Plotting of tensile strength, rupture strain and (B) toughness of the hydrogels against R_{PEA}

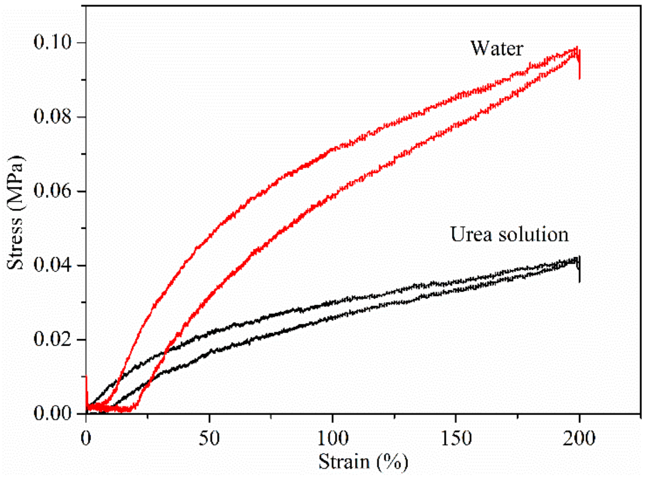

Figure S8 the loading-unloading curves of the hydrogel P20-A80 after treatment in urea solution and water, respectively.

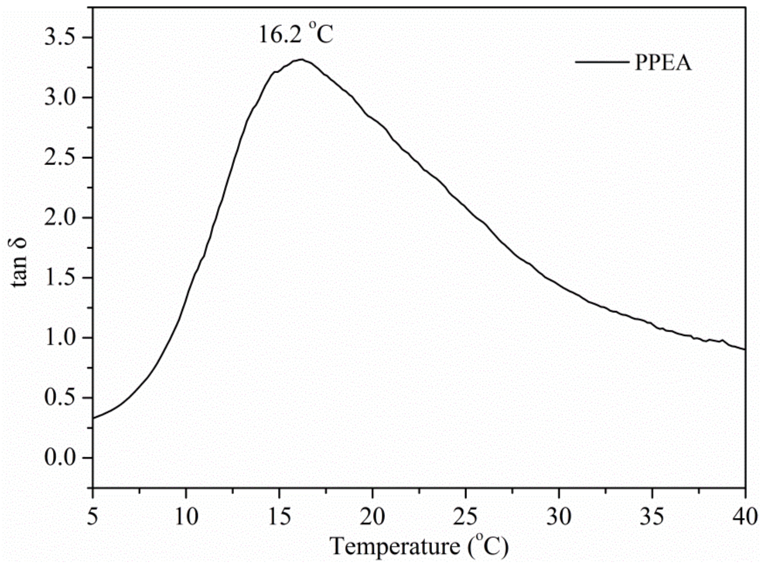

Figure S9 The loss factor (tan δ) as a function of temperature for PPEA. The peak value of 16.2 °C was used to denote the T_g of the PPEA.

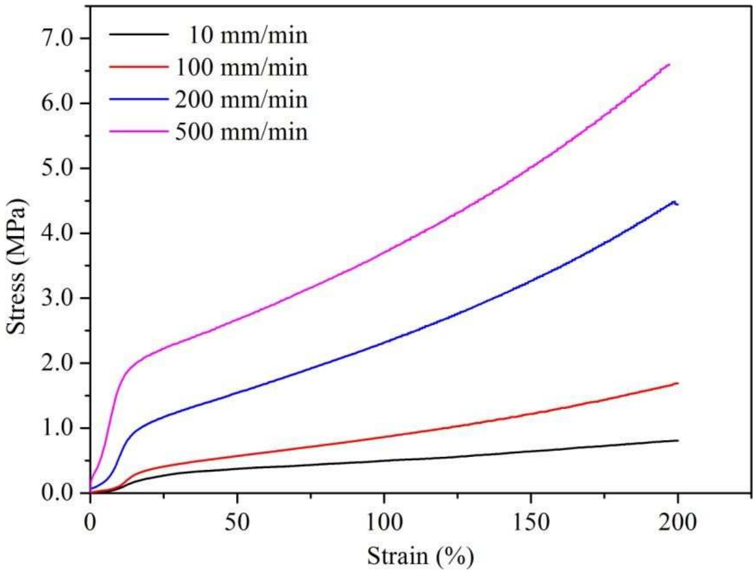

Figure S10 The deformation-rate dependence of mechanical behavior for P60-A40 hydrogel. The maximum tensile strain was fix at 200%.

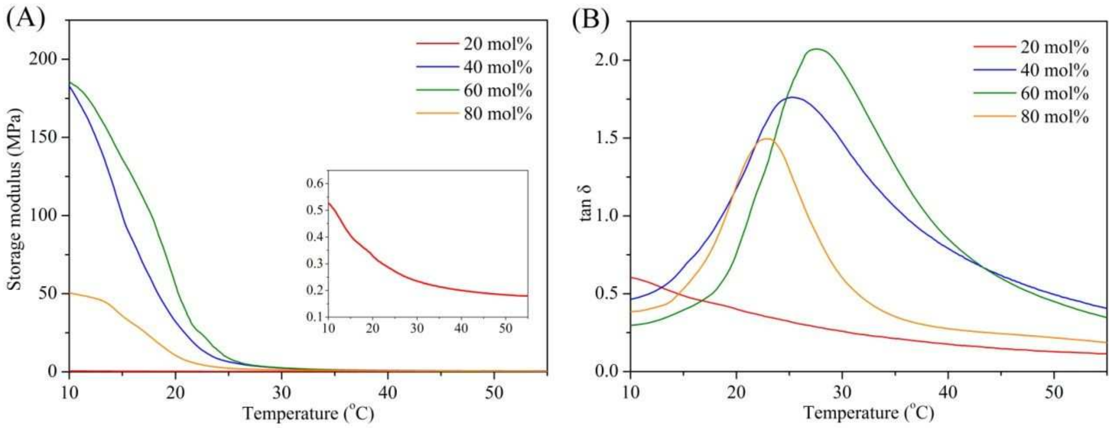

Figure S11 The (A) storage moduli and (B) loss factors (tan δ) of hydrogels with R_{PEA} ranging from 20 to 80 mol% as a function of temperature.

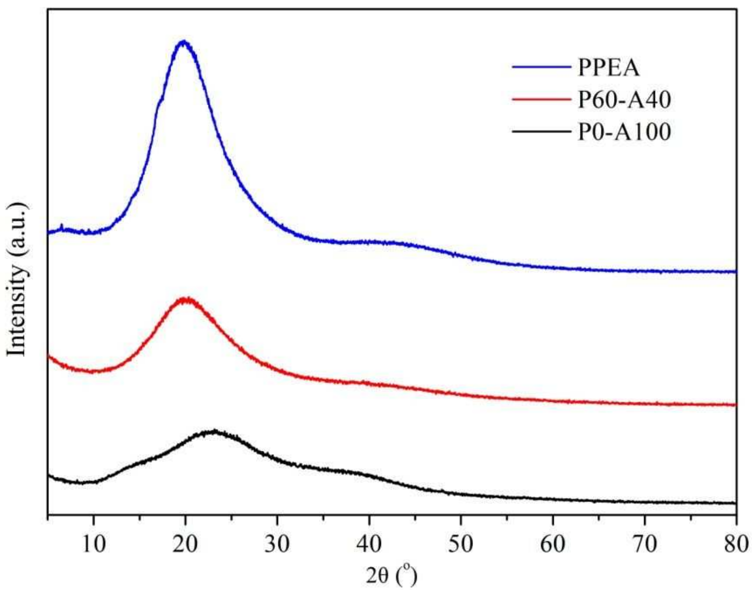

Figure S12 The WAXD patterns of the dried P0-A100, P60-A40 hydrogels and PPEA.

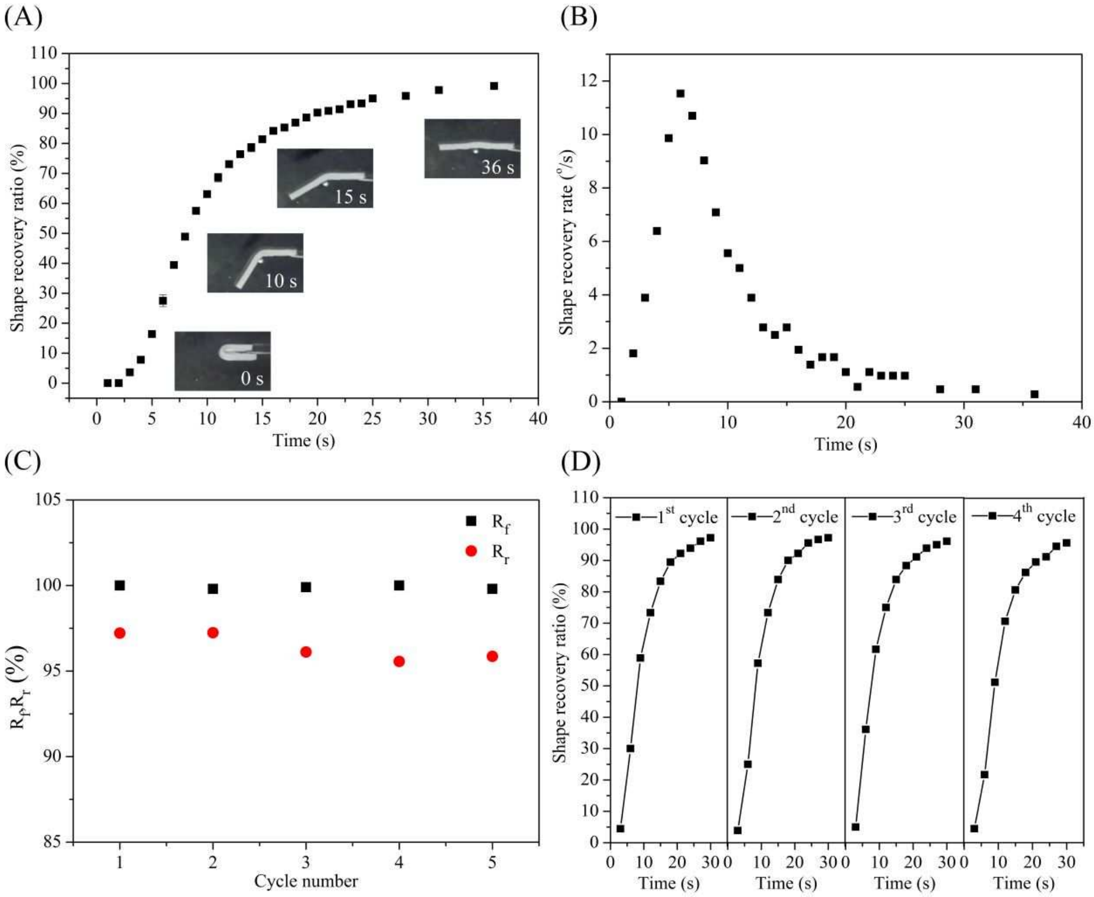

Figure S13 Quantitative evaluation of the body temperature-responsive shape memory performance of the hydrogel P60-A40. A strip-shaped hydrogel sample was fixed at a temporary U-shape through cooling (10 ^{o}C), followed by shape recovery in response to body temperature (37 ^{o}C). (A) Shape recovery process of P60-A40 hydrogel over time. (B) The shape recovery rate of P60-A40 hydrogel as a function of recovery time. (C) R_f and R_r of the hydrogel which were determined during cyclic evaluation. (D) Cyclic shape memory behavior of the hydrogel.

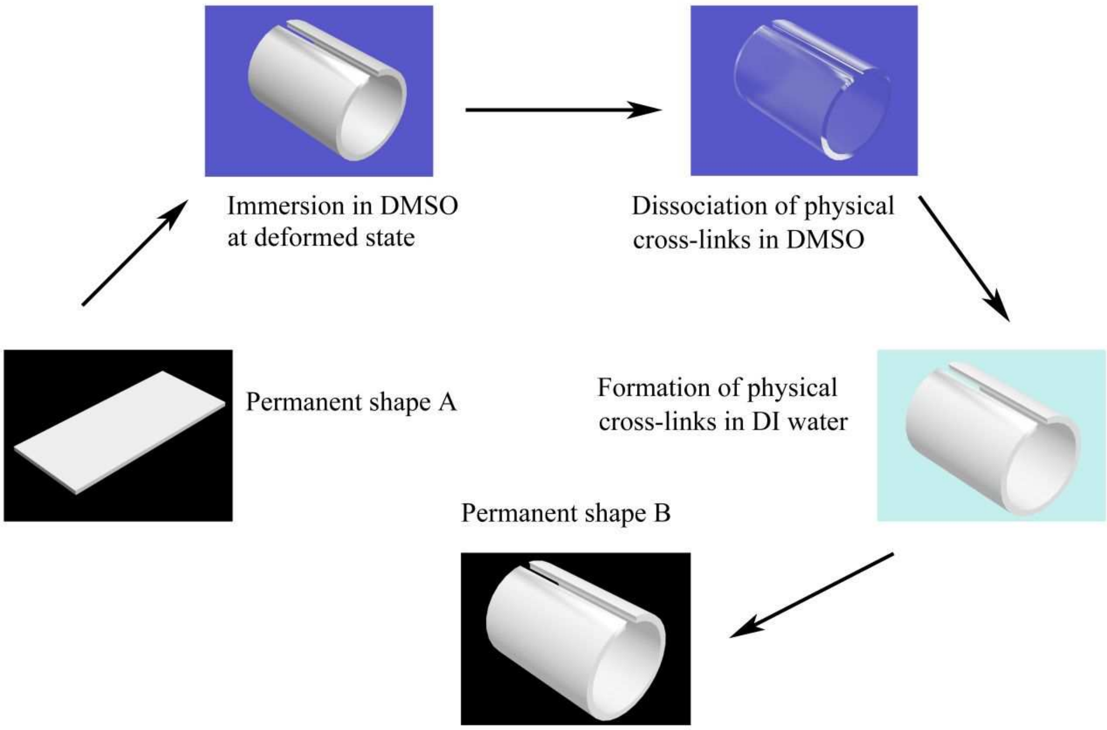

Figure S14 Schematic illustration of the permanent shape re-programming process through the DMSO-H_2O treatment.

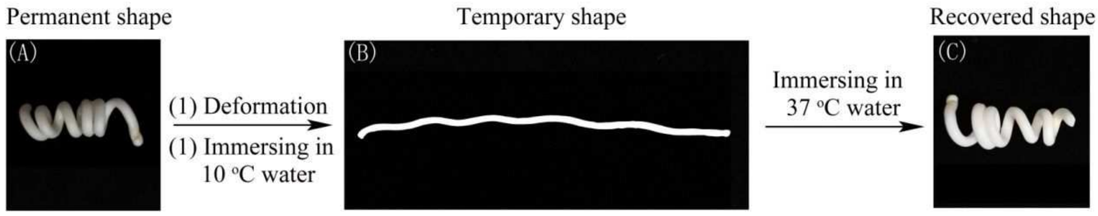

Figure S15 Shape memory behavior of the reprogrammed permanent shape (A) P60-A40 hydrogel strip with the reprogrammed coiled permanent shape; (B) the linear temporary shape was fixed by successive heating in 37 ºC water, applying force and cooling in 10 ºC water; (C) shape recovery of the coiled shape in 37 ºC water.

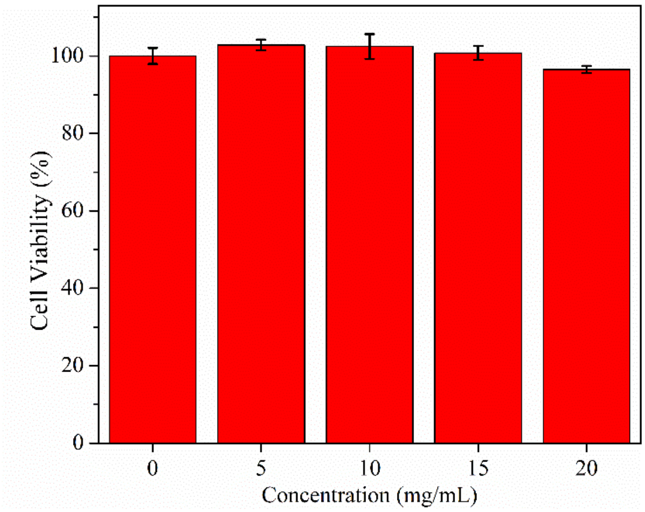

Figure S16 Cytocompatibility evaluation of the hydrogel P60-A40. All the hydrogel extracts with concentration varying from 0 to 20 presented a cell viability higher than 95%, indicating no cytotoxic content leached from the hydrogel network.

Table S1 the recipe for preparing the poly (PEA-*co*-AAm) and poly(PEA-*co*-DMAA) hydrogels

No.	PEA		AAm		DMAA		PEGDA700		DMSO	ABVN	
	mg	mmol	mg	mmol	mg	mmol	mg	mmol	ml	mg	mmol
P0-A100	0	0	4548	64.0	0	0	23.0	0.033	11.6	32.1	0.13
P10-A90	1230.1	6.4	4096.1	57.6	0	0	22.8	0.033	11.1	32.2	0.13
P20-A80	2460.6	12.8	3642.8	51.2	0	0	22.6	0.032	10.5	31.9	0.13
P40-A60	4921.9	25.6	2729.4	38.4	0	0	22.9	0.033	9.0	32.1	0.13
P50-A50	6156.5	32.0	2276.2	32.0	0	0	22.3	0.032	8.0	32.1	0.13
P60-A40	7391.0	38.5	1814.7	25.5	0	0	23.0	0.033	7.7	31.6	0.13
P80-A20	9840.0	51.2	908.1	12.8	0	0	22.8	0.033	6.5	31.5	0.13
P20-D80	1545.2	8.0	0	0	3171.1	32.0	14.2	0.02	5.0	19.6	0.08
P60-D40	4621.0	24.0	0	0	1590.3	16.0	14.1	0.02	4.5	19.5	0.08

Table S2 the recipe for preparing the poly (BzA-*co*-AAm) and poly(PEMA-*co*-AAm) hydrogels

No.	BzA		PEMA		AAm		PEGDA700		DMSO	ABVN	
	mg	mmol	mg	mmol	mg	mmol	mg	mmol	ml	mg	mmol
Poly (BzA-co-AAm)	2146.3	13.2	0	0	1364.9	19.2	11.1	0.016	5.3	15.9	0.064
Poly (PEMA-co-AAm)	0	0	1316.4	6.4	1820.6	25.6	11.3	0.016	5.3	15.8	0.064

Table S3 Parameters of typical shape memory behavior and mechanical property of thermal-responsive SMHs reported in recent years

Entry	Mechanism of shape memory effect	Trigger temperature	Tensile strength	Rapture strain	R_f	R_r	Recovery time
		^{o}C	MPa	%	%	%	s
Poly (PEA-co-AAm) hydrogel (this work)	association/ dissociation of hydrophobic interaction and hydrogen bonding	37	5.1±0.16	368.7±17.4	100%	>95	36
Poly(vinylpyrrolidone-*co*-acryloxy acetophenone) hydrogel [2]	association/ dissociation of hydrophobic interaction /π-π stacking	60-80	1.54-8.40	26	100	74-89	8-180
PVA-TA hydrogel [3]	formation/ breakage of hydrogen bonding	60	2.88-3.57	<1100	50-70	~100	5
FOSM side chain hydrogel [4]	formation/ breakage of hydrogen bonding	65	0.27−0.54	500−580	76.3-98.3	~100	N/A
Organohydrogel [5]	melting-crystallization transition	45-70	N/A	>2600	100	60-100	40
PVA-PEG double network hydrogel [6]	melting/ crystallization of crystalline microdomain	90	0.7-1.3	300-400	76-90	N/A	>15
Poly(MAAc-*co*-NVP-*co*-PEGMA) hydrogel [7]	hydrogen bonding	50	3.9	600	N/A	N/A	~30

SA-SH/PVA hydrogel [8]	melting/ crystallization of crystalline microdomain	90	N/A	N/A	40	95	120
Agarose/poly(AA-*co*-AAc) interpenetrating network hydrogel [9]	coil-helix transformation of agarose	70	N/A	N/A	~100	95.6	50
PAN-PAAm-PEG3kDMA hydrogel [10]	disassociation/association of dipole-dipole interaction and hydrogen bonding	37	12	~1000	97.5	100	4
Gelatin/GO/PAAm interpenetrating double network hydrogel [11]	coil-helix transition of gelatin chain	80	0.1-0.4	400-1600	0-80	N/A	N/A
DMAA-*co*-MAAc hydrogel [12]	formation/ breakage of hydrogen bonding	50	<2	400-850	N/A	~100	15
Physical A11AUA-based hydrophobically associated hydrogel [13]	association/ dissociation of hydrophobic interaction	60	0.017-0.89	1864-8508	N/A	N/A	~14
Biphasic Synergistic hydrogel [14]	melting-crystallization transition	40-80	0.42-0.93	100-230	100	100	N/A

Table S4 The composition, mechanical properties and body temperature-responsive SME of hydrogels prepared with AAm and different hydrophobic monomers

Hydrogels	Hydrophobic monomer ratio	Young's modulus	Rupture strain	Tensile strength	Soften temperature	R_f at 10 °C	R_r at 37 °C	Time at 37 °C
	(mol. %)	MPa	%	MPa	°C	%	%	s
Poly (BzA-co-AAm)	40	9.01±1.38	377.2±36.8	2.36±0.14	26.69	>98.0	>98.0	30±2
Poly (PEMA-co-AAm)	20	4.38±0.45	199.9±7.3	1.98±0.02	37.45	93.3±1.7	>98.0	54±4

Legends for Supplementary Movies

Movie S1： Two halves of the DMSO-swollen P60-A40 hydrogel samples were brought into contact for several seconds but no connection was observed.

Movie S2: The two halves of the DMSO-swollen P60-A40 hydrogel sample were welded rapidly after immersing into DI water for several seconds.

Movie S3: The body temperature responsiveness of the P60-A40 hydrogel.

Movie S4: The body temperature triggered shape memory performance of the P60-A40 hydrogel sample with a reprogrammed coiled permanent shape.

Movie S5: The *in vitro* embolization assessment of the P60-A40 sample using a customized flow system.

Reference

(1) Bai, Y. K.; Zhang, J. W.; Chen, X. A Thermal-, Water-, and near-Infrared Light-Induced Shape Memory Composite Based on Polyvinyl Alcohol and Polyaniline Fibers. *ACS Appl. Mater. Interfaces* **2018,** *10* (16), 14017-14025.

(2) Jiao, C.; Chen, Y.; Liu, T.; Peng, X.; Zhao, Y.; Zhang, J.; Wu, Y.; Wang, H. Rigid and Strong Thermoresponsive Shape Memory Hydrogels Transformed from Poly(Vinylpyrrolidone-Co-Acryloxy Acetophenone) Organogels. *ACS Appl. Mater. Interfaces* **2018,** *10* (38), 32707-32716.

(3) Chen, Y.; Peng, L.; Liu, T.; Wang, Y.; Shi, S.; Wang, H. Poly (Vinyl Alcohol)–Tannic Acid Hydrogels with Excellent Mechanical Properties and Shape Memory Behaviors. *ACS Appl. Mater. Interfaces* **2016,** *8* (40), 27199-27206.

(4) Hao, J.; Weiss, R. Mechanically Tough, Thermally Activated Shape Memory Hydrogels. *ACS Macro Lett.* **2013,** *2* (1), 86-89.

(5) Zhao, Z.; Zhang, K.; Liu, Y.; Zhou, J.; Liu, M. Highly Stretchable, Shape Memory Organohydrogels Using Phase-Transition Microinclusions. *Adv. Mater.* **2017,** *29* (33), 1701695.

(6) Li, G.; Zhang, H.; Fortin, D.; Xia, H.; Zhao, Y. Poly (Vinyl Alcohol)–Poly (Ethylene Glycol) Double-Network Hydrogel: A General Approach to Shape Memory and Self-Healing Functionalities. *Langmuir* **2015,** *31* (42), 11709-11716.

(7) Xu, C.; Tang, Q.; Yang, H. Y.; Peng, K.; Zhang, X. Y. High-Strength, Thermally Activated Shape Memory Hydrogels Based on Hydrogen Bonding between Maac and Nvp. *Macromol. Chem. Phys.* **2018,** *219* (10), 7.

(8) Tang, L.; Wen, L.; Xu, S.; Pi, P.; Wen, X. Ca 2+, Redox, and Thermoresponsive Supramolecular Hydrogel with Programmed Quadruple Shape Memory Effect. *Chem. Commun.* **2018,** *54* (58), 8084-8087.

(9) Peng, K.; Yang, K.; Fan, Y.; Yasin, A.; Hao, X.; Yang, H. Thermal/Light Dual ‐ Activated Shape Memory Hydrogels Composed of an Agarose/Poly (Acrylamide ‐ Co ‐ Acrylic Acid) Interpenetrating Network. *Macromol. Chem. Phys.* **2017,** *218* (17), 1700170.

(10) Zhang, Y.; Gao, H.; Wang, H.; Xu, Z.; Chen, X.; Liu, B.; Shi, Y.; Lu, Y.; Wen, L.; Li, Y. Radiopaque Highly Stiff and Tough Shape Memory Hydrogel Microcoils for Permanent Embolization of Arteries. *Adv. Funct. Mater.* **2018,** *28* (9), 201705962.

(11) Huang, J.; Zhao, L.; Wang, T.; Sun, W.; Tong, Z. Nir-Triggered Rapid Shape Memory Pam-Go-Gelatin Hydrogels with High Mechanical Strength. *ACS Appl. Mater. Interfaces* **2016,** *8* (19), 12384-12392.

(12) Hu, X. B.; Vatankhah-Varnoosfaderani, M.; Zhou, J.; Li, Q. X.; Sheiko, S. S. Weak Hydrogen Bonding Enables Hard, Strong, Tough, and Elastic Hydrogels. *Adv. Mater.* **2015,** *27* (43), 6899-+.

(13) Wei, D.; Yang, J.; Zhu, L.; Chen, F.; Tang, Z.; Qin, G.; Chen, Q. Semicrystalline Hydrophobically Associated Hydrogels with Integrated High Performances. *ACS Appl. Mater. Interfaces* **2018,** *10* (3), 2946-2956.

(14) Zhao, Z.; Liu, Y.; Zhang, K.; Zhuo, S.; Fang, R.; Zhang, J.; Jiang, L.; Liu, M. Biphasic Synergistic Gel Materials with Switchable Mechanics and Self ‐ Healing Capacity. *Angew. Chem. Int. Ed.* **2017,** *56* (43), 13464-13469.